

Microphase State of Oligobutadienediol-Based Polyurethaneureas

YU. S. LIPATOV, N. V. DMITRUK, V. V. TSUKRUK, and V. V. SHILOV,
*The Institute of Macromolecular Chemistry, Academy of Sciences,
Ukrainian SSR, 252160 Kiev, USSR* and L. S. PRISS, and L. I.
DASHEVSKY, *The Research Institute of Tyre Industry, 117321 Moscow,
USSR*

Synopsis

Structural studies of oligobutadienediol-based polyurethanes with various degrees of crosslinking were carried out. From absolute small-angle X-ray scattering, the degree of segregation of components was determined. It was concluded that a complete microphase separation of the different components is realized in all samples irrespective of the degree of crosslinking, and these polymers are two-phase systems. While stretching, the fibrillar structure is formed.

INTRODUCTION

The processes of microphase separation exert considerable influence on physicochemical and mechanical properties of polyblock polymers.¹ It can be fully referred to polyurethane elastomers in which the presence of alternating soft and hard fragments results in the microphase separation of different components.^{2,3} The degree of component segregation determining the completeness of phase separation varies with the nature of macromolecular fragments over a wide range. The completeness of phase separation is greatly influenced by a degree of polymer crosslinking.^{4,5}

At present the studies on the synthesis of polyurethanes based on oligodiols of diene nature are fast progressing. But the structure of such polymers has not practically been studied. In this connection we have performed studies on the microphase state of some oligobutadienediol-based urethaneureas with hard fragments of different nature and a different degree of crosslinking.

MATERIALS AND METHODS

Polyurethaneureas were synthesized on the basis of oligobutadienediols with a molecular weight of 3000, obtained by radical polymerization 1,3'-butadiene with 4,4'-azobis(4-cyanopentanol) as initiator.⁶ The use of this hydroxyl-containing initiator allows us to obtain oligobutadienediols with a high degree of bifunctionality and a narrow molecular weight distribution. The synthesis was performed in two stages: macrodiisocyanate was prepared by reaction of oligobutadienediol with 2,4-toluylenediisocyanate at a 2:1 molar ratio of NCO to OH; then the macrodiisocyanate was crosslinked with the formation of polyurethaneurea. 3,3'-Dichlor-4,4'-diaminodiphenylmethane (samples of D series) and a mixture of 4,4'-diaminodiphenylmethane and 4,4',4''-triaminotriphenylmethane (samples of DT series) were used as structure-forming agents.

TABLE I
 Sample Characteristics

Sample	Molar ratio		Hard fragment content (%)	Equilibrium degree of swelling in chloroform (%)
	NH ₂ /NCO	Diamine/triamine		
D-0.8	0.8/1.0	—	15.9	650
D-1.0	1.0/1	—	17.1	1700
DT-1.0/0	1.0/1	1.0/0	15.5	3000
DT-0/0.67	1.0/1	0/0.67	15.4	600

For the first series the crosslinking was conducted in bulk at 120°C. The crosslinking was performed by the reaction of an abundance of isocyanate groups with forming biuretic and allophanic links. The network density was changed by varying a ratio of NH₂ to NCO over the range of 0.6–1.2. For the second series due to high amine reactivity crosslinking was performed in dioxan solution at room temperature, with the solvent being removed from polymer films. The degree of crosslinking was determined by a molar ratio of diamine to triamine which was varied over the range of 1.0/0–0/0.67. A ratio of NH₂ to NCO was always equal to 1.0. The time of crosslinking calculated from the highest degree of conversion of reactive groups was 5–6 h.

The polyurethaneureas characteristics and data on their equilibrium swelling in chloroform are given in Table I. For structural X-ray diffraction studies the samples with a maximum degree of crosslinking (D-0.8 and DT-0/0.67) as well as very weakly crosslinked, practically linear samples with a maximum extended of oligomer chains (D-1.0 and DT-1.0/0) were chosen.

WAXS measurements were made on a diffractometer based on a URS-2.0 generator (automatic step-by-step scanning, nickel filter, proportional counter, pulse-height analyzer). SAXS and WAXS photopatterns of oriented samples were obtained on a KRM-1 unit with a special WAXS attachment.⁷

SAXS measurements were made on a Rigaku-Denki type diffractometer (nickel filtered Cu radiation, scintillation counter, pulse-height analyzer).⁸ A step of automatic scanning was 0.02°. The subtraction of air scattering background was performed according to a known procedure.⁹ To reduce to the absolute intensity units, a standard Kratky sample was used. A full treatment of small-angle curves, including smoothing, subtraction of wide-angle scattering, reduction to absolute intensity, calculation of mean square of electron density fluctuation, and calculation of correlation functions, was conducted according to Vonk's procedure.¹⁰ The detailed description of a SAXS experiment is given in a monograph.⁹

The electron density fluctuation $\Delta\bar{\rho}^2$ was determined from the small-angle scattering invariant Q :

$$Q = 4\pi \int S^2 \mathbf{I}(s) ds \quad (1)$$

$$\Delta\bar{\rho}^2 = K \cdot Q \quad (2)$$

where $s = 2 \sin \theta / \lambda$, θ is the half-angle, λ is the wavelength, and K is the calibration factor.

The theoretical values of $\Delta\bar{\rho}_i^2$, assuming the complete separation of compo-

nents, were calculated proceeding from the oligobutadienediol density $\rho_2 = 0.90$ g/cm³ and the densities of compounds modelling hard fragments $\rho_1 = 1.30$ g/cm³ (for DT) and $\rho_2^1 = 1.43$ g/cm³ (for D).

The degree of component segregation, α , characterizing the completeness of phase separation, was evaluated from the relationship

$$\alpha = \Delta\bar{\rho}^2 / \Delta\bar{\rho}_i^2 \quad (3)$$

where $\Delta\bar{\rho}_i^2 = \varphi(1 - \varphi)(\rho_1 - \rho_2)^2$, φ the volume fraction of one of the components.

The correlation functions characterizing the distribution of electron density in a system were calculated by the Fourier transform of the scattering curve:

$$\gamma_3(r) = \frac{1}{l} \int \mathbf{T}(s) \sin(sr) ds \quad (4)$$

RESULTS AND DISCUSSION

For all the polyurethaneurea samples of D and DT series diffuse wide-angle scattering and one well-defined small-angle peak are observed at about 1° (Figs. 1 and 2; Table II). The interplanar spacings corresponding to the small-angle peak for the polymers investigated are given in Table II.

SAXS curves for the D-1.0, D-0.8, DT-1.0/0, and DT-0/0.67 samples are presented in Figure 1; WAXS curves for those samples are given in Figure 2. One diffuse maximum on WAXS curves is indicative of the amorphous structure of polyurethaneureas studied. The practically identical shape and position of maxima for different samples are mainly associated with the scattering from the regions of soft fragment packing taking up to 90% of the bulk of a polymer. Since

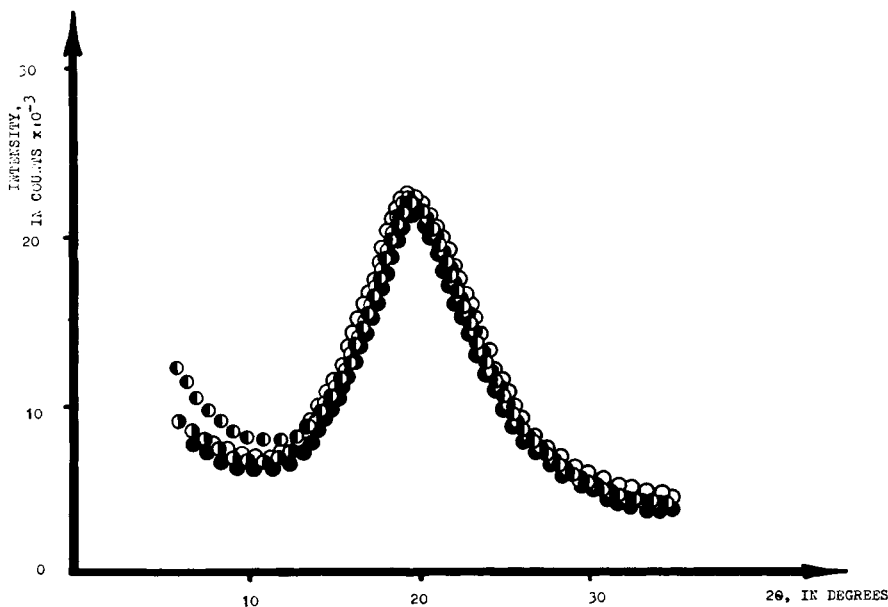


Fig. 1. SAXS intensity curves: (●) 1, D-1.0; (◐) 2, D-0.8; (○) 3, DT-1.0/0; (◑) 4, DT-0/0.

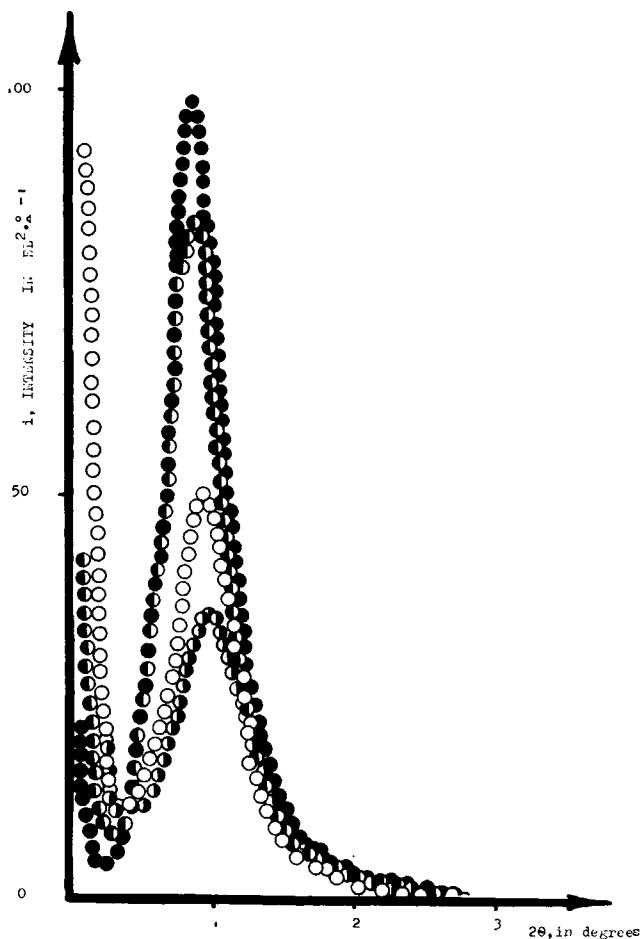


Fig. 2. WAXS intensity curves (symbols are defined in Fig. 1).

the nature of soft fragments is not changed, it is quite natural that the shape and position of a wide-angle maximum remain unchanged.

The intense small-angle scattering with the peak corresponding to a spacing of 70–80 Å is observed for all the samples. First of all, it is indicative of the heterogeneity of the polymers investigated. Here microregions with different electron density form a macrolattice with a well-pronounced distance between adjacent crosslinks. Such microregions can be formed due to the aggregation of hard segment blocks, this phenomenon being quite usual for block polymer

TABLE II
Structural Parameters of Polyurethaneureas

Sample	d (Å)	$\Delta\bar{\rho}^2$ (el/Å ³) ²	$\Delta\bar{\rho}_i^2$ (el/Å ³) ²	α (%)
D-0.8	85	1.8×10^{-3}	2.5×10^{-3}	75
D-1.0	83	1.9×10^{-3}	2.5×10^{-3}	73
DT-1.0/0	76	1.1×10^{-3}	1.4×10^{-3}	74
DT-0/0.67	70	1.1×10^{-3}	1.4×10^{-3}	79

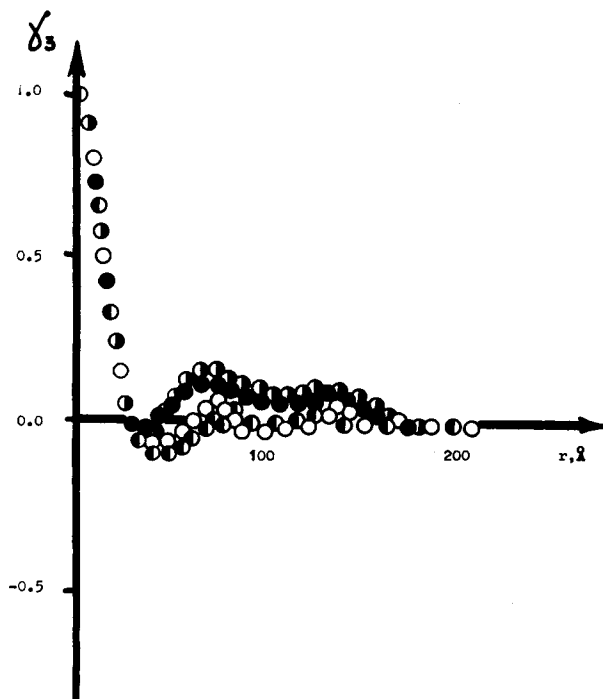


Fig. 3. Spherically symmetric correlation functions $\gamma_3(r)$ (symbols are defined in Fig. 1).

systems.⁹ In this case the intensity and position of the small-angle peak characterize the degree of macrolattice order, its crosslinks being hard segment domains dissolved in the soft segment matrix.

A comparison of macrolattice spacings and distances between adjacent hard fragments along the molecular chain, calculated for the Kuhn segment of an oligobutadienediol fragment at a fully extended conformation of a hard fragment, points to an approximate equality of these values. Thus the macrolattice spacing for the polymers studied can really be associated with the distance between adjacent domains containing macromolecular hard fragments.

The spherically symmetric correlation functions $\gamma_3(r)$ of electron density distribution have one well-defined peak at 70–80 Å and a very weak maximum at 140–170 Å (Fig. 3). It shows that considerable deviations of local density from the macroscopic one outside the second coordination sphere are absent. It is apparently associated with the fact that the lattice is paracrystalline and has no long-range order in the arrangement of hard segment domains.

The position of a small-angle peak is identical for the two polymers D-1.0 and D-0.8 (84 Å); for the two other polymers of DT series it decreases to 76 Å. The peak intensity of the polymer D-1.0 is 20% higher than that of the sample D-0.8, and the peak intensity of DT-1.0/0 is 35% higher than that of DT-0/0.67. Besides, the intensity of small-angle scattering for the polymers of D series is much higher than the intensity for the samples of DT series. The latter can be explained by the presence of the chlorine atoms in the hard fragments of the polymer of D series. These atoms have much higher scattering power as compared with the carbon or oxygen atoms.

The polymers D-1.0 and D-0.8 differ mainly in the degree of crosslinking of hard fragments. If in D-1.0 the macromolecules are successively alternating hard and soft fragments without any branching, in D-0.8 about 25% of hard fragments are three-functional crosslinks of the network. As mentioned earlier, the small-angle peak intensity in a crosslinked polymer is 20% lower as compared with a linear analog. Taking into account the nature of a small-angle peak, one can draw the conclusion that the degree of order in the arrangement of hard segment domains becomes lower with the increase in the network density. It is apparently caused by far greater steric hindrances appearing in a crosslinked polymer, when the network of chemical bonds is formed, preventing the hard segment domains from being more perfectly dissolved in the soft segment matrix.¹¹

A similar picture is observed for the polymers DT-1.0/0 and DT-0/0.67 as well, the decrease of the small-angle peak intensity being much more pronounced (25%). It is probably associated with a much higher density of the network of chemical bonds in a crosslinked polymer.

To quantitatively evaluate the completeness of microphase separation in block and multicomponent systems, the degree of component segregation, α , is used.^{2,9,11} We calculated the value of α for the polymers investigated proceeding from the invariant Q , the volume fraction of different components φ_1 and φ_2 , the packing density of hard and soft fragments ρ_1 and ρ_2 . The value of α for various polymers differs inconsiderably and is within 70–80% (Table 2). Such high values of α , as is known,^{9,11} are characteristic of the systems with almost full phase separation of components. The fact that α does not reach maximum values (100%) can be explained by the presence of transition zones between hard segment domains and the soft segment matrix and, on the other hand, by the some degree of mixing of different components.^{11–13} As is known, the mean square of electron density fluctuation $\Delta\bar{\rho}^2$ is connected with the presence of transition zones with E thickness in a complicated way¹⁴:

$$\Delta\bar{\rho}^2 = (\rho_1 - \rho_2)^2(\varphi_1\varphi_2 - ES/6V) \quad (5)$$

where S is the surface and V is the volume of domain.

In simplest case of lamellar form of domains these relation may be rewritten (for details see Ref. 15):

$$\Delta\bar{\rho}^2 = (\rho_1 - \rho_2)^2(\varphi_1\varphi_2 - \varphi_3/6) \quad (6)$$

where φ_3 is the volume fraction of the transition zone.

Simple calculations show that, to decrease the degree of segregation from 100% to 80%, it is enough that the volume fraction of transition zone was about 10–20%. When an average distance between domains in macrolattice is about 80 Å, the thickness of a transition zone should be 8–16 Å. Thus the decreasing of α in our polymers may be connected with the presence of the transition zones only, but not with mixing of components of different nature. In such sense in investigated systems a full phase separation of different fragments of macromolecules is realized (without mixing of components but with presence of transition zones). It is a specific feature of oligobutadienediol-based polyurethaneureas. For conventional polyurethane systems⁹ with polyester soft fragments, the value of α can rarely reach 60%. It can probably be associated with the fact that the polyoxyolefin soft fragments in these systems are apt to specifically interact with

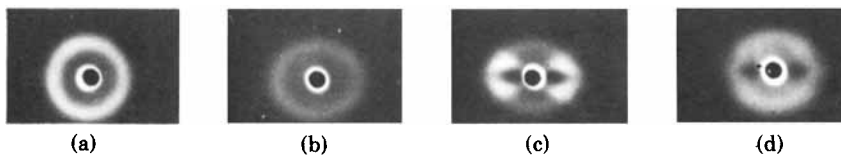


Fig. 4. (1)

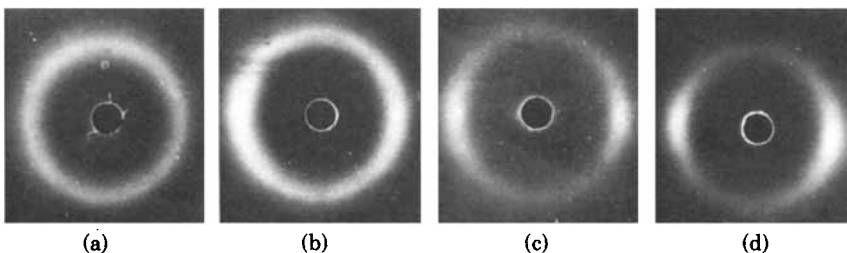


Fig. 4. (2)

Fig. 4. SAXS and WAXS photopatterns for the polymers: D-1.0 (1) and DT-1.0/0 (2). Degree of stretching, λ : (a) 1; (b) 1.3; (c) 3; (d) 6.

hard fragments. This contributes to the increase in compatibility of different components and, therefore, to the decrease of the degree of component segregation.¹³ Thus, the absence of specific interactions between urethaneurea hard segment blocks and oligobutadiene soft fragments in the systems investigated should lead to the increase in incompatibility of components. This, in its turn, contributes to the completeness of phase separation, which causes the increase in the degree of component segregation to the maximum possible values.

From structural transformations while stretching one can determine the dimensional characteristics of hard segment domains. In this connection we studied elongation of polyurethaneureas samples as a function of stretching $\lambda = l/l_0$ to 6–8 (l_0 is the length of the unstretched sample; l is the length of the sample after stretching). The changes in X-ray photopatterns with the increase in λ are slightly different for various polymers. Typical WAXS and SAXS photopatterns for one of the samples are given in Figure 4. As can be seen from this figure, at low degrees of stretching ($\lambda = 1.3$), the initial isotropic ring on the SAXS photopattern is transformed into the ellipse with the major axis directed along the equator; i.e., here the increase in spacing along the direction of orientation d_{\parallel} and its decrease in transverse direction are taking place d_{\perp} . As is known, in case of affine deformation the variations of d_{\parallel} and d_{\perp} obey the conditions

$$\begin{aligned} d_{\parallel} &= \lambda d_0 \\ d_{\perp} &= d_0/\sqrt{\lambda} \end{aligned} \quad (7)$$

where d_0 is the spacing for the isotropic sample.

For all the polymers investigated the variations of λ during stretching differ by 10–20% from the macroscopic deformation, i.e., the deformation is not an affine one. The absence of affinity at early stages of deformation can be associated both with the inhomogeneity of the macrolattice in the bulk of the sample and with the deviation of the shape of hard segment domains from the spherically

symmetric one.¹⁶ Really, in the case of anisodiametrically shaped hard segment domains, the lower microscopic deformation as compared with the macroscopic one is determined by the processes of additional orientation of hard segment domains at the knots of the macrolattice.

The increase in the degree of stretching to $\lambda = 3$ leads to considerable changes of scattering patterns: SAXS photopatterns have reflexes of radial type with an azimuthal spread of 30–40°, weak diffuse scattering can be seen at the meridian (Fig. 4). Proceeding from the photopatterns, one may say that oriented polymers tilted structures, with longitudinal domain sizes being 1.5–2 times higher than their cross sizes, exist.¹⁷ The angle of radial reflex splitting is 40–80°; i.e., the angle of domain deviation from the axis of orientation is within 20–40°. The spacing can be evaluated from the arrangement of dash reflexes at the equator of the photopattern. They are within 50–60 Å.

A further increase in the degree of stretching results in a higher degree of domain orientation along the direction of stretching; thus the final structure at $\lambda = 6-8$ is a typical fibrillar structure with spacings of 110 Å and 50–60 Å along the axis of orientation and in the transverse direction, respectively. Here both hard and soft fragments are oriented along the direction of stretching, and the equatorial position of a wide-angle reflex confirms this fact (Fig. 4).

CONCLUSIONS

Examining the data obtained, one may note the following peculiarities of structural state of polyurethaneureas.

In all the samples investigated a complete microphase separation of different components with maximum possible degrees of segregation up to 100% is realized irrespective of the chemical crosslinking of macromolecular fragments. Thus all the polymers are two-phase systems. This is a peculiarity of the systems under study as opposed to conventional polyurethanes based on polyoxyolefin fragments. It can be connected with the increase in incompatibility of different components due to the absence of specific interactions between them.

Then, the chemical crosslinking of hard fragments results in a lower degree of order in the arrangements of hard segment domains because of the increase in steric hindrances.

Hard segment domains dissolved in the soft segment matrix are anisodiametrically shaped. When the degree of polymer stretching increases to $\lambda > 3$, the structural rearrangement takes place with the formation of a fibrillar structure. Here the hard and soft fragments are arranged along the direction of stretching.

References

1. A. Noshay and J. E. McGrath, *Block Copolymers*, Academic, New York, 1977.
2. R. Bonart and E. Müller, *J. Macromol. Sci. B*, **10**, 345 (1974).
3. C. S. Paik Sung, C. D. Hu, and C. S. Wu, *Am. Chem. Soc., Polym. Prepr.*, **19**, 679 (1978).
4. Z. Ophir and G. L. Wilkes, in *Multiphase Polymer Symposium*, Anaheim, Calif., March 1978, American Chemical Society, Washington, D.C., 1979, p. 53.
5. *Polyurethane Chemistry Successes*, Yu. S. Lipatov, Ed., Naukova Dumka, Kiev, 1972 (in Russian).
6. A. E. Kalas, Z. E. Kogan, I. B. Belov, and M. E. Breskina, *Kautshuk Rezina*, **12** (7), 7 (1974) (in Russian).

7. V. V. Vorona and T. M. Gritsenko, *Pribory Techn. Exp.*, to appear (in Russian).
8. N. I. Sosfenov, L. A. Fejgin, K. P. Bondarenko et al., *Apparatura Metody Rent. Analys.*, No. 5, 53 (1969) (in Russian).
9. Yu. S. Lipatov, V. V. Shilov, Yu. P. Gomza, and N. E. Kruglyak, *X-Ray Methods of Polymer System Investigation*, Naukova Dumka, Kiev, 1982 (in Russian).
10. C. G. Vonk, *J. Appl. Crystallogr.*, **8**, 340 (1975).
11. Yu. S. Lipatov and V. V. Shilov, *Kompoz. Polym. Mater.*, No. 11, 55 (1981) (in Russian).
12. *Polymer Blends*, D. Paul and S. Newman, Eds., Academic, New York, 1978, Vol. 2.
13. Yu. S. Lipatov, *Interphase Phenomena in Polymers*, Naukova Dumka, Kiev, 1980 (in Russian).
14. C. G. Vonk, *J. Appl. Crystallogr.*, **6**, 81 (1973).
15. F. H. Khambata, F. Walker, P. Russel, R. S. Stein, *J. Polym. Sci., Polym. Phys. Ed.*, **14**, 1391 (1976).
16. E. J. Roche, R. S. Stein, T. P. Russel, and W. J. MacKnight, *J. Polym. Sci., Polym. Phys. Ed.*, **18**, 1497 (1980).
17. V. J. Gerasimov, Ya. V. Genin, and D. Ya. Tsvankin. *J. Polym. Sci., Polym. Phys. Ed.*, **12**, 2035 (1974).

Received February 25, 1983

Accepted October 7, 1983

Corrected proofs received March 26, 1984